Theoret. Chim. Acta (Berl.) 59, 25–45 (1981)

THEORETICA CHIMICA ACTA

Chemical Applications of Group Theory and Topology. X. Topological Representations of Hyperoctahedrally Restricted Eight-Coordinate Polyhedral Rearrangements [1]

R. Bruce King

Department of Chemistry, University of Georgia, Athens, GA 30602, USA

The hyperoctahedral wreath product group $P_4[P_2]$ of order 384 spans the symmetries of the chemically important eight coordinate polyhedra (cube, hexagonal bipyramid, D_{2d} dodecahedron, and square antiprism) as well as the fully symmetric group P_8 of order $8! = 40320$. This restriction by a factor of 105 makes the treatment of permutational isomerizations of eight-coordinate polyhedra tractable for the first time. In connection with such a treatment this paper describes the isomers of those four eight-coordinate polyhedra which can be obtained by restricting the permutations of the vertex labels to the $P_4[P_2]$ group. A topological representation of the interconversions between enantiomeric pairs of these hyperoctahedrally restricted isomers of the eight-coordinate polyhedra consists of a $K_{4,4}$ bipartite graph with hexagons at its eight vertices. The eight vertices of the $K_{4,4}$ graph correspond to cubes, the total of 48 vertices on the eight hexagons correspond to the square antiprisms, the 48 edges of the hexagons correspond to the D_{2d} dodecahedra, and the 16 edges of the original $K_{4,4}$ graph correspond to the hexagonal bipyramids. The lowest energy process interconverting eight coordinate polyhedra consists of paths around the circumference of a given hexagon corresponding to interconversions between D_{2d} dodecahedra and square antiprisms which do not require the cube or hexagonal bipyramid as intermediates. The following two additional features of the hyperoctahedral restrictions on the vertex permutations of the eight coordinate polyhedra are of some significance: (1) The hyperoctahedral restriction removes processes in D_{2d} dodecahedra and square antiprisms involving enantiomer interconversion thereby suggesting that such processes have higher energies and leading to the prediction of optically stable fluxional eight-coordinate complexes; (2) Since $P_4[P_2]$ is a

0040-5744/81/0059/0025/$04.20

soluble group in contrast to P_8 which is not soluble, the hyperoctahedrally restricted permutations between the isomers of the individual polyhedra have a natural group structure which disappears when the hyperoctahedral restrictions are removed.

Key words: Polyhedral rearrangements – Eight-coordinate complexes – Topological representations – Permutation group theory – Hyperoctahedral wreath product groups – Permutational isomerizations.

1. Introduction

During the past fifteen years the chemistry and spectroscopy of stereochemically non-rigid [2–4] or fluxional [5] molecules has received considerable attention. Of particular interest are polyhedral rearrangements [6, 7] in coordination complexes of the type ML_n (M = central atom, most frequently a metal; L = ligands). The cases of five [8–17] and six [18–24] coordinate polyhedra have received extensive consideration. Topological representations [6, 7] of polyhedral rearrangements have been developed for these systems. Thus rearrangements in five-coordinate polyhedra with non-chelating ligands can be represented as a double group pentagonal dodecahedron [6], Petersen's graph, [15, 25] or the Desargues–Levi graph [10, 26]. Similarly, rearrangements in six-coordinate complexes can be represented as a pentagonal dodecahedron [18], the Desargues–Levi graph [26, 27] or a seven-dimensional analogue of the tetrahedron (K_8 graph) [22].

Considerably less progress has been made in the development of topological representations for rearrangements in polyhedra with more than six vertices. The difficulty in the treatment of such systems has been their large *isomer counts* [6] which range from 504 to 10 080 for the commonly encountered seven- and eight vertex polyhedra. This paper presents a new approach for the analysis of polyhedral rearrangements in eight vertex polyhedra. This approach selects from the unmanageable number of eight-vertex polyhedral permutational isomers a well-defined manageable subset (the *hyperoctahedrally restricted subset*) of these isomers. This subset is topologically closed [6] with respect to internal isomerizations which appear sufficient to represent interconversions of eight-coordinate polyhedra other than interconversion of enantiomers.

2. Some Relevant Concepts in Graph Theory and Group Theory

Since topological representations [6, 7] are graphs, some relevant concepts in graph theory [28] will first be reviewed in order to provide a foundation for the understanding of some of the specific points discussed in this paper. A *graph* is defined [28] as a finite non-empty set V together with a (possibly empty) set E (disjoint from V) of two-element subsets of (distinct) elements of V. Each element of V is called a vertex and V itself is called the vertex set of G. The members of the edge set E are called edges. The edge $e = \{u, v\}$ is said to join the vertices u and v. If $e = \{u, v\}$ is the edge of a given graph, then u and v are called *adjacent* vertices.

A polyhedron is simply a graph that is realizable in three-dimensional Euclidean space. (More precisely a graph is a 1-*skeleton* [29] of a polyhedron.) A *topological representation* is a graph representing permutational isomerizations [30] in which the vertices represent different permutational isomers and the edges represent processes of a specified type for isomer interconversion.

Group theory [31, 32] is useful for analyzing the symmetry properties of graphs in a way completely analogous to the use of point groups [28] for analyzing the symmetry of three-dimensional polyhedra. Thus the *automorphism group* [29, 30] of a graph is the group of permutations of its vertices which preserves the adjacency relationships of the vertices. The automorphism groups of graphs correspond to the point groups of three-dimensional polyhedra. The concepts of a graph and its automorphism group are thus generalizations of the concepts of a polyhedron and its point group where the requirement of realizability in three-dimensional space is removed. A graph realizable as the 1-skeleton of a three-dimensional polyhedron can be drawn on a piece of paper without any crossing edges. Such a graph is called a planar graph [28], other graphs are non-planar graphs.

A fundamental theorem in graph theory [33] states that any permutation group can be the automorphism group of some graph although not necessarily a graph with as few vertices as the number of objects interchanged by the permutation group. In any case a permutation group of interest can be depicted as the minimum vertex graph having the permutation group as its automorphism group.

The largest group permuting n objects is the fully symmetric group represented here as P_n (for consistency with a previous paper [34] of this series where the more conventional designation [32] S_n is inconvenient because of the possibility for confusion with improper rotations [31] also designated S_n). The group P_n contans $n!$ elements representing all possible permutations of n objects. The minimum vertex graph $G_{\min}(P_n)$ of which P_n is the automorphism group is the *complete graph* [28, 35] K_n which consists of n vertices with an edge connecting every possible pair of vertices. The graph K_n thus has $n(n-1)/2$ edges.

The *isomer count* I of a polyhedron with n vertices is $n!/|R|$ where $|R|$ is the order of the rotational subgroup of the point group of the polyhedron [6, 7]. This counts the number of distinguishable permutational isomers [7, 30] of the polyhedron in question. For the eight-coordinate polyhedra $n! = 40320$, which means that the cube, hexagonal bipyramid, square antiprism, and D_{2d} dodecahedron have isomer counts of $40320/24 = 1680$, $40320/12 = 3360$, $40320/8 = 5040$, and $40320/4 = 10080$, respectively. A graph corresponding to a topological representation of permutational isomerizations involving such large numbers of polyhedral isomers is clearly unwieldy and unmanageable.

The problem of representing permutational isomerizations [7, 30] in eight-coordinate polyhedra can be simplified if a subgroup of P_8 is found which contains the symmetries of all of the polyhedra of interest. A previous paper of this series [34] shows that the wreath product group [36–40] $P_4[P_2]$ of order 384 contains all of the symmetries of the cube, hexagonal bipyramid, square antiprism, and D_{2d}

dodecahedron which are all of the eight-coordinate polyhedra [41] of interest. If the group $P_4[P_2]$ rather than P_8 is used to calculate *restricted isomer counts* $2J = 384/|R|$, the more manageable isomer counts of 16, 32, 48, and 96 are obtained for the cube, hexagonal bipyramid, square antiprism, and D_{2d} dodecahedron, respectively. These $2J$ isomer counts are now small enough that topological representations of the interconversions of these isomers are feasible.

The concept of restricting permutations of ligands in eight-coordinate ML_8 complexes to those in the wreath product group $P_4[P_2]$ rather than in the fully symmetric P_8 group can be restated in graph theoretical terms using the hyperoctahedral graph [35] H_4. Therefore such a restriction of permutations from P_8 to $P_4[P_2]$ will be called a *hyperoctahedral restriction*. The hyperoctahedral graphs underlying this restriction are designated as H_n and have $2n$ vertices with every vertex connected to all except one of the remaining vertices so that each vertex of H_n is of degree $2(n-1)$. (The name "hyperoctahedral" comes from the fact that an H_n graph is the 1-skeleton of the analogue of the octahedron (the "cross-polytope") in n-dimensional space [26].) Thus H_2 and H_3 correspond to the square and the octahedron, respectively. The automorphism group of H_n is the corresponding wreath product group $P_n[P_2]$ of order $2^n(n!)$. Thus the $P_4[P_2]$ wreath product group of interest in this paper is the automorphism group of H_4 which is the 1-skeleton of the four-dimensional analogue of the octahedron (the "cross-polytope" γ_4) [29]. This hyperoctahedral graph H_4 has 8 vertices, 24 edges, and each vertex is of degree 6 (i.e. connected to 6 edges). There are therefore only four *unconnected* pairs of vertices in H_4. The *standard labelling* of H_4 can be defined without loss of generality to give the four unconnected vertex pairs the number pairs 1 and 2, 3 and 4, 5 and 6, and 7 and 8. These pairs of unconnected vertices in the standard labelling of the H_4 hyperoctahedral graph are conveniently called *trans complements* by analogy with the standard designation of *trans* positions in octahedra.

These graph theoretical concepts can be related to the isomer counts defined above through the concept of graph coverings. Such graph coverings consider only pairs of connected graphs having *equal numbers* of vertices. Label such a pair of connected graphs as G_1 and G_2 so that G_1 has at least as many edges as G_2. An *admissible covering* of G_1 by G_2 involves superimposing the vertices of G_1 and G_2 so that each edge of G_2 falls on an edge of G_1. Two admissible coverings C_1 and C_2 of G_1 by G_2 may be considered *distinguishable* if C_1 covers different edges of G_1 than C_2. Thus if G_1 and G_2 have the same numbers of edges as well as the same numbers of vertices the number of admissible coverings of G_1 by G_2 must be either 1 or 0. For example, the number of distinguishable admissible coverings of G_1 by G_2 where G_2 is a polygon (with the same number of vertices as G_1) corresponds to the number of distinguishable Hamiltonian circuits [28] in G_1.

The various isomer counts can now be expressed in terms of graph coverings. Thus the conventionally defined isomer count $\mathrm{I} = n!/|R|$ (i.e. relative to the fully symmetric permutation group P_n) for a polyhedron with n vertices corresponds to the number of distinguishable admissible coverings of the 1-skeleton of the polyhedron on the complete graph K_n. Analogously, the hyperoctahedrally restricted isomer count for eight-vertex polyhedra $2J = 384/|R|$ (i.e. relative to $P_4[P_2]$ rather than P_8) corresponds to the number of distinguishable admissible coverings of the 1-skeleton of the polyhedron on the hyperoctahedral graph H_4. The isomers of an eight vertex polyhedron counted by $2J$ and represented by such distinguishable admissible coverings of H_4 are called *hyperoctahedrally restricted permutational isomers*. If the underlying hyperoctahedral graph H_4 is given the standard labeling as defined above, hyperoctahedrally restricted permutational isomers of eight vertex polyhedra cannot have edges between the four pairs of trans complements, i.e. vertices 1 and 2, vertices 3 and 4, vertices 5 and 6, vertices 7 and 8. This is the essential feature that is used to select the hyperoctahedrally restricted permutational isomers of the eight vertex octahedra from all possible permutational isomers of the eight vertex octahedra (i.e. those representable as distinguishable admissible coverings of K_8).

The following features of the hyperoctahedrally restricted permutational isomers are also of interest:
(1) Eight vertex polyhedra will always have fewer edges than the hyperoctahedral graph H_4. Thus whereas H_4 has 24 edges, the maximum number of edges possible for an eight vertex polyhedron [42] is 18 corresponding to an eight vertex polyhedron containing only triangular faces (e.g. the hexagonal bipyramid or the dodecahedron). Thus in a hyperoctahedrally restricted permutational isomer of an eight-vertex polyhedron, there will be other pairs of vertices besides the *trans* complements which are unconnected by edges. In effect, the different ways of choosing these additional unconnected vertices which are not *trans* complements lead to the multiplicity of hyperoctahedrally restricted permutational isomers for a given polyhedron.
(2) If an eight vertex polyhedron has $2J$ hyperoctahedrally restricted permutational isomers, these isomers can be represented as J pairs of enantiomers conveniently called *hyperoctahedrally restricted enantiomeric pairs*. Thus the cube, hexagonal bipyramid, square antiprism, and D_{2d} dodecahedron have 8, 16, 24, and 48 hyperoctahedrally restricted enantiomeric pairs, respectively.
This paper describes the hyperoctahedrally restricted enantiomeric pairs of the four eight-vertex polyhedra of interest in terms of their vertex labels relative to the standard labelling of the underlying H_4 graph as defined above. Topological representations of permutation isomerization reactions between these hyperoctahedrally restricted enantiomeric pairs can then be presented for the first time.

A valid question at this point is to what extent do permutational isomerization reactions between hyperoctahedrally restricted enantiomeric pairs of eight-coordinate polyhedra reflect permutational isomerizations that actually take place in real systems where there need not be hyperoctahedral restrictions. In other words, what price do we pay for simplifying the eight coordinate permutational isomerization problem by a factor of $40320/384 = 105$ in terms of the number of permutational isomers? In this connection the following comments pertain:
(1) The wreath product group $P_4[P_2]$ contains all of the symmetries of the eight coordinate polyhedra of interest. However, because of a special feature of the

square antiprism to be discussed in detail later, a direct product group $P_4[P_2] \times C_2$ of order $(384)(2) = 768$ is required to contain sufficient symmetries to allow interconversions between the D_{2d} dodecahedron and the D_{4d} square antiprism with the minimum vertex displacements. This direct product group may be considered as a *double group* [26, 31, 43] analogous to those which have various chemical and physical applications. Interestingly enough, this double group $P_4[P_2] \times C_2$ unlike $P_4[P_2]$ is *not* a subgroup of P_8 since 40320/768 is not an integer.
(2) Most significantly, the hyperoctahedral restriction, as modified by double group formation, leads to topological representations based on relatively simple graphs for conversions between the eight vertex polyhedra.
(3) The hyperoctahedral restriction appears to remove spatially reasonable processes for enantiomer interconversion at least in the lowest energy eight-coordinate polyhedra. This is why J pairs of enantiomers are considered rather than $2J$ individual isomers. This suggests that fluxional processes [5] leading, for example, to the interconversion of D_{2d} dodecahedral isomers and making all eight vertices equivalent on an n.m.r. time scale [44] will be of lower inherent energy than racemization of optically active eight coordinate complexes. Although extensive information is avilable on eight-coordinate complexes [41], experiments designed to test this point do not yet seem to have been performed.

3. Properties of Eight-Coordinate Polyhedra

Table 1 summarizes the properties of the four eight-coordinate polyhedra of interest in this work. These polyhedra are depicted in Fig. 1 along with examples of hyperoctahedrally acceptable labellings. The lattice of subgroups [40] of P_8

Table 1. Properties of the eight-coordinate polyhedra

Polyhedron	Edges	Vertices[a] j_3	j_4	j_5	j_6	Faces[b] t	q	Point group[c] G	$\lvert G\rvert$	Isomer counts[d] I	J	Cycle index (multiplied by $\lvert G\rvert$)
Cube	12	8	0	0	0	0	6	O_h	48	1680	8	$x_1^8+8x_1^2x_3^2+13x_2^4+12x_4^2+8x_2x_6+6x_1^4x_2$
Hexagonal bipyramid	18	0	6	0	2	12	0	D_{6h}	24	3360	16	$x_1^8+2x_1^2x_6+7x_1^2x_2^3+2x_1^2x_3^2+4x_2^4+2x_2x_3^2+2x_2x_6+x_1^6x_2+3x_1^4x_2^2$
Dodecahedron	18	0	4	4	0	12	0	D_{2d}	8	10080	48	$x_1^8+2x_1^4x_2^2+3x_2^4+2x_4^2$
Square antiprism	16	0	8	0	0	8	2	D_{4d}	16	5040	24	$x_1^8+4x_1^2x_2^3+5x_2^4+2x_4^2+4x_8$

[a] j_n refers to the number of vertices of degree n (i.e. with n edges meeting at the vertex).
[b] t refers to the number of triangular faces; q refers to the number of square or quadrilateral faces.
[c] G refers to the point group; $|G|$ refers to the number of elements in the point group.
[d] $I = 8!/|R|$ where $|R|$ is the size of the rotational subgroup of G ($=|G|/2$ in these cases); $J = 384/|G|$. See text.

relevant to this paper is given in Fig. 2, where the orders of each of the groups are given in parentheses. Solid arrows connect a group with its subgroups accessible through chains of normal subgroups [32]; if no such normal subgroup chain exists (e.g. $P_8 \rightarrow P_4[P_2]$), the arrow is dotted. The numbers above the arrows in Fig. 2 correspond to the indices of the subgroups.

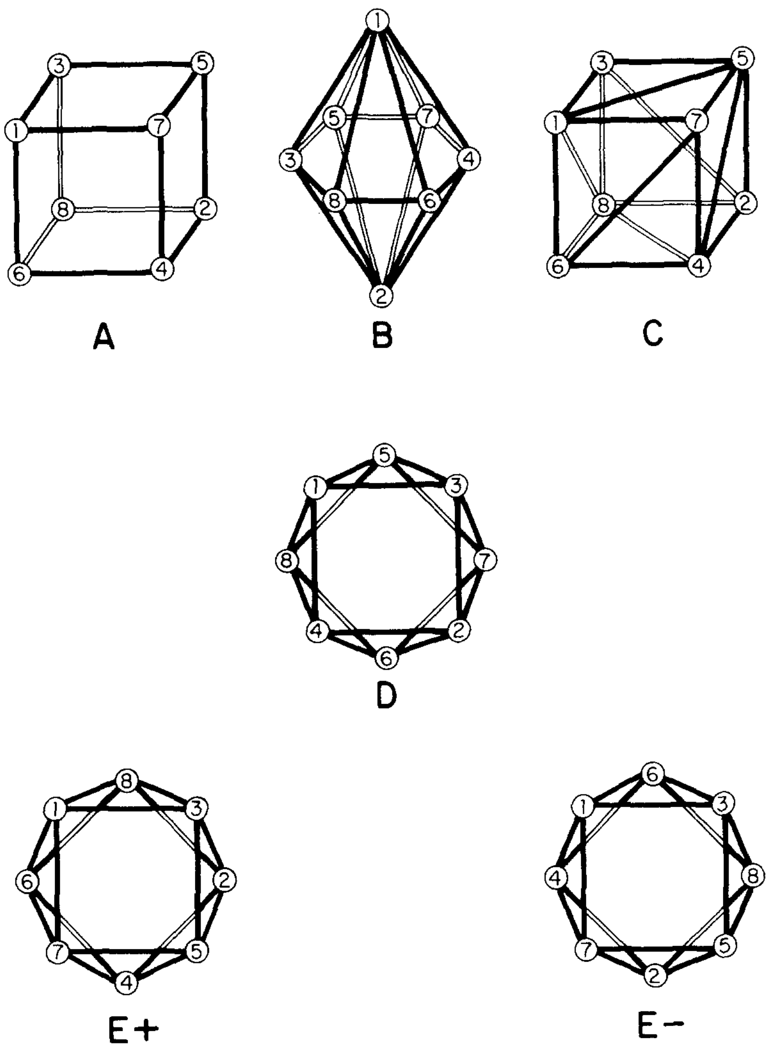

Fig. 1. Examples of eight-coordinate polyhedra considered in this paper with examples of hyperoctahedral restrictions: (**a**) The hyperoctahedrally restricted cube 1–367–458–2 (or 367); (**b**) The hyperoctahedrally restricted hexagonal bipyramid 12–357468; (**c**) The 1-skeleton of the hyperoctahedrally restricted D_{2d} dodecahedron 15, 54, 48, 81, 23, 67 depicted as the underlying cube 1–367–458–2 with the four added primary diagonals and the two added secondary diagonals; (**d**) A possible hyperoctahedrally restricted square antiprism but not one conforming to the rules developed in this paper as being useful for depicting permutational isomerizations; (**e**+ and **e**−): The two antipodally related hyperoctahedrally restricted square antiprisms 1357–8246 and 1357–6824

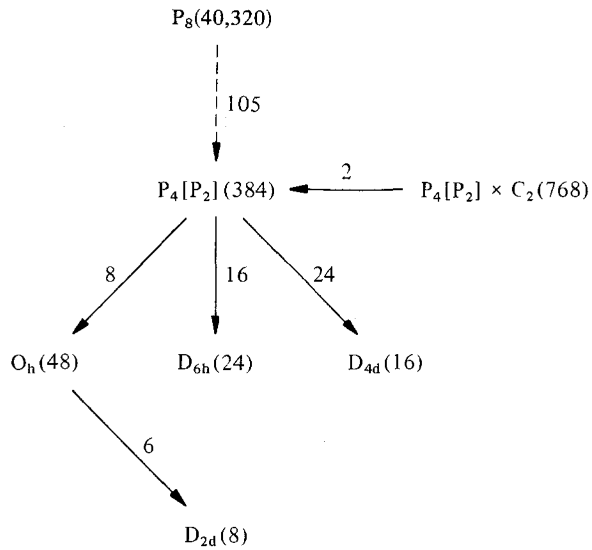

Fig. 2. Lattice of subgroups relevant to this paper between the fully symmetric group P_8 and the D_{2d}, D_{4d}, and D_{6h} point groups. Solid arrows connect a group with its subgroups reachable by a normal chain whereas a dotted arrow connects the simple P_8 group with its largest subgroup considered here $P_4[P_2]$. The indices of the subgroups are indicated over the arrows

The following summarizes the essential features of these polyhedra and their hyperoctahedrally acceptable labellings;

1. Cube. A given vertex of a cube has three adjacent vertices, three vertices two edges away at opposite vertices of the face diagonals, and one vertex three edges away at the opposite vertex of the body diagonal. A hyperoctahedrally restricted labelling of a cube can be described as $1\text{–}b_1c_1d_1\text{–}b_2c_2d_2\text{–}2$ (or more concisely as $b_1c_1d_1$) where $b_1c_1d_1$ represents the three vertices adjacent to 1 and b_1 and b_2, c_1 and c_2, and d_1 and d_2 are the three pairs of *trans* complements other than the 1, 2 pair. Thus the labelling in Fig 1a can be represented as 1–368–457–2 or more concisely as 368. The *trans* complements 1 and 2, 3 and 4, 5 and 6, and 7 and 8 are situated at the ends of the four body diagonals of the cube when its labelling is hyperoctahedrally restricted in the standard manner.

2. Hexagonal bipyramid. A hyperoctahedrally restricted labelling of a hexagonal bipyramid can be described as $a_1a_2\text{–}b_1c_1d_1b_2c_2d_2$ where: (a) a_1a_2 represents the two apices; (b) $b_1c_1d_1b_2c_2d_2$ represents a path around the equatorial hexagon; (c) a_1 and a_2, b_1 and b_2, c_1 and c_2, and d_1 and d_2 represent the four pairs of *trans* complements. Thus the labelling in Fig. 1b can be represented as 12–345678. The *trans* complement vertex pairs 1 and 2, 3 and 4, 5 and 6, and 7 and 8 are located at opposite apices and at the three pairs of opposite equatorial vertices ("para positions") of the hexagonal bipyramid when its labelling is hyperoctahedrally restricted in the standard manner.

3. D_{2d} dodecahedron. The 1-skeleton of a D_{2d} dodecahedron can be constructed from that of an underlying cube by adding six new edges. These new edges are face diagonals of the underlying cube as follows:

(a) Four *primary diagonals* along a *belt* of four faces to form a cycle of length four along these four diagonals (e.g. 15, 54, 48, 81 in Fig. 1c along a belt containing the top, right, bottom, and left faces in that order).

(b) Two *secondary diagonals* along the remaining two faces to form the characteristic interpenetrating tetrahedra of the D_{2d} dodecahedron. One of these tetrahedra has all vertices of degree five and the other tetrahedron has all vertices of degree four.

Since D_{2d} is a subgroup of O_h a D_{2d} dodecahedron with 18 edges may be considered as a cube which is distorted so that the additional six face diagonal edges have approximately the same length as the twelve original cube edges. Six different D_{2d} dodecahedra can be formed from a given cube depending on how the new face diagonal edges are added relating to the fact that D_{2d} is a subgroup of index six in O_h. These dodecahedra can be designated by listing first the four primary diagonals and then the two secondary diagonals. Thus the D_{2d} dodecahedron in Fig. 1c is formed from the cube in Fig. 1a and can be designated as 15, 54, 48, 81, 23, 67.

4. Square antiprism. A hyperoctahedrally restricted square antiprism in principle could be constructed by locating the four *trans* complement vertex pairs at the ends of the four diagonals of the two square faces (e.g. *D* in Fig. 1). However, such a hyperoctahedrally restricted square antiprism cannot be converted to the hyperoctahedrally restricted versions of the other eight vertex polyhedra constructed as above through reasonable processes for polyhedral rearrangements. Therefore, this procedure for generating hyperoctahedrally restricted square antiprisms is of little value in studying rearrangements in eight coordinate polyhedra.

In order to avoid this difficulty a completely different procedure is used to construct a different type of hyperoctahedrally restricted square antiprism which can occur in hyperoctahedrally restricted polyhedral rearrangements involving square antiprisms. This procedure uses a 45° twist of opposite faces of a hyperoctahedrally restricted cube defined as outlined above. Since a cube has three disjoint opposite pairs of square faces and since the 45° twist can be applied in either of two directions, six different square antiprisms can be generated from a given underlying cube. Thus in Fig. 1 the square antiprisms $E+$ and $E-$ can be generated from cube A by twisting the 1357 and 2468 faces 45° relative to each other but in opposite directions. An alternative method of considering hyperoctahedrally restricted square antiprisms of this type is to require that the *trans* complement vertex pairs 1 and 2, 3 and 4, 5 and 6, and 7 and 8 are each situated at a given vertex and a corresponding *antipodal* vertex. In this connection two vertices of a square antiprism are defined as an antipodal pair of vertices if they are on opposite square faces and are *not* connected by a single edge. Since a given vertex of a square antiprism has *two* such antipodal vertices, the number of hyperoctahedrally restricted square antiprismatic *enantiomeric pairs* generated in this manner is $2J$ rather than J. This process of generating hyperoctahedrally restricted square antiprisms is analogous to using the $P_4[P_2]\times C_2$ direct product group of degree $(384)(2)=768$ rather than the $P_4[P_2]$ group as the spanning group for rearrangements involving square antiprisms. The new C_2 factor of this direct product group relates to whether the opposite faces of the underlying cube are twisted clockwise or counterclockwise in forming the corresponding square antiprism. Since $|P_8|/|P_4[P_2]|=105$ is an odd number, the direct product or double group $P_4[P_2]\times C_2$ cannot be a subgroup of P_8 by Lagrange's theorem [31, 32].

The numberings of these hyperoctahedrally restricted square antiprisms correspond to $1b_1c_1d_1$–$d_22b_2c_2$ or $1b_1c_1d_1$–$c_2d_22b_2$ depending upon the direction of twist of the opposite pair of square faces of the underlying cube. Again b_1 and b_2, c_1 and c_2, and d_1 and d_2 correspond to the three pairs of *trans* complements other than the 1, 2 pair.

The relationships between the various hyperoctahedrally restricted eight-vertex polyhedra and their standard labellings are given in Tables 2 and 3. Table 2 gives the standard labellings as defined above representing the 8 cube and the 16 hexagonal bipyramid hyperoctahedrally restricted enantiomeric pairs. Table 3 lists the standard labellings of the hyperoctahedrally restricted enantiomeric pairs of the 48 D_{2d} dodecahedra and the 48 D_{4d} square antiprisms generated from the 8 cube enantiomeric pairs. Note that in this system of labelling of eight vertex polyhedra the partitioning of the vertex labels uniquely defines the polyhedron: a cube has a 1, 3, 3, 1 (or 3) partition of labels, a hexagonal bipyramid has a 2, 6 partition of labels, a D_{2d} dodecahedron has a 2, 2, 2, 2, 2, 2 partition of labels, and a square antiprism has a 4, 4 partition of labels.

The following additional features of the four eight-coordinate polyhedra are of chemical interest and relevant to the treatment in this paper:
(1) The D_{2d} dodecahedron and the square antiprism have much lower interligand repulsion energies than the cube and hexagonal bipyramid [41].

Table 2. Hyperoctahedrally acceptable labellings of the cube and hexagonal bipyramid[a]

A. Cube			
1–357–468–2	1–457–368–2	1–367–458–2	1–467–358–2
1–358–467–2	1–458–367–2	1–368–457–2	1–468–357–2
B. Hexagonal bipyramid			
12–357468	34–157268	56–317428	78–351462
12–367458	34–167258	56–327418	78–361452
12–358467	34–158267	56–318427	78–352461
12–368457	34–168257	56–328417	78–362451

[a] Each of these labellings represents a pair of enantiomers. See text.

Table 3. D_{2d} dodecahedra and square antiprisms corresponding to hyperoctahedrally acceptable labellings of the cube

				Cube			
1–357–468–2	1–457–368–2	1–367–458–2	1–467–358–2	1–358–467–2	1–458–367–2	1–368–457–2	1–468–357–2
(A) Square Antiprisms (48)							
1385–7624	1485–7623	1386–7524	1486–7523	1375–8624	1475–8623	1376–8524	1476–8523
1385–6247	1485–6237	1386–5247	1486–5237	1375–6248	1475–6238	1376–5248	1476–5238
1367–5824	1467–5823	1357–6824	1457–6823	1368–5274	1468–5723	1358–6724	1458–6723
1367–8245	1467–8235	1357–8246	1457–8236	1368–7245	1468–7235	1358–7246	1458–7236
1547–3826	1537–4826	1647–3825	1637–4825	1548–3726	1538–4726	1648–3725	1638–4725
1547–8263	1537–8264	1647–8253	1637–8254	1548–7263	1538–7264	1648–7523	1638–7254
(B) D_{2d} Dodecahedra (48)							
14, 48, 86, 61	13, 38, 86, 61	14, 48, 85, 51	13, 38, 85, 51	14, 47, 76, 61	13, 37, 76, 61	14, 47, 75, 51	13, 37, 75, 51
27, 35	27, 45	27, 36	27, 46	28, 35	28, 45	28, 36	28, 46
25, 53, 37, 72	25, 54, 47, 72	26, 63, 37, 72	26, 64, 47, 72	25, 53, 38, 82	25, 54, 48, 82	26, 63, 38, 82	26, 64, 48, 82
14, 68	13, 68	14, 58	13, 58	14, 67	13, 67	14, 57	13, 57
14, 46, 68, 81	13, 36, 68, 81	14, 45, 58, 81	13, 35, 58, 81	14, 46, 67, 71	13, 36, 67, 71	14, 45, 57, 71	13, 35, 57, 71
25, 37	25, 47	26, 37	26, 47	25, 38	25, 38	26, 38	26, 48
23, 37, 75, 52	24, 47, 75, 52	23, 37, 76, 62	24, 47, 76, 62	23, 38, 85, 52	24, 48, 85, 52	23, 38, 86, 62	24, 48, 86, 62
18, 46	18, 36	18, 45	18, 35	17, 46	17, 36	17, 45	17, 35
16, 64, 48, 81	16, 63, 38, 81	15, 54, 48, 81	15, 53, 38, 81	16, 64, 47, 71	16, 63, 37, 71	15, 54, 47, 71	15, 53, 37, 71
23, 57	24, 57	23, 67	24, 67	23, 58	24, 58	23, 68	24, 68
23, 35, 57, 72	24, 45, 57, 72	23, 36, 67, 72	24, 46, 67, 72	23, 35, 58, 82	24, 45, 58, 82	23, 36, 68, 82	24, 46, 68, 82
16, 48	16, 38	15, 48	15, 38	16, 47	16, 37	15, 47	15, 37

(2) In an ML_8 complex the D_{2d} dodecahedron and the square antiprism can be formed by sp^3d^4 hybridization of the central atom M whereas formation of the cube and hexagonal bipyramid must involve the f orbitals as well as the s, p, and d orbitals of M [42]. For these reasons the D_{2d}-dodecahedron and the square antiprism are much more favorable coordination polyhedra than the cube and hexagonal bipyramid. Therefore polyhedral isomerization processes involving only D_{2d} dodecahedra and square antiprisms are of lower energy and therefore more favored than such processes also involving the cube and/or hexagonal bipyramid.

4. Hyperoctahedrally Allowed Interconversion of Eight Coordinate Polyhedra

The following three types of interconversions of eight coordinate polyhedra are possible under hyperoctahedral restrictions as defined above:

A. Interconversion between the cube (O_h) and the hexagonal prism (D_{6h}) (the O_h–D_{6h}–O_h process in Fig. 3a). In this process a *trans* complement vertex pair of the cube (i.e. a pair along a body diagonal such as vertices 1 and 2 in Fig. 3a) is selected to be the *pivot vertices.* The remaining six vertices of the cube become coplanar in the hexagonal bipyramidal intermediate. Further movement of these vertices in the same direction leads ultimately to a new cube in which the three vertices adjacent to one pivot vertex in the original cube become adjacent to the other pivot vertex in the new cube and vice versa. The permutation cycle structure (analogous to a cycle index term in a permutation group [36–39]) of this process is $x_1^2x_2^3$ where the factor x_1^2 refers to the two "fixed" pivot vertices. This permutation is an odd process (i.e. the sum of exponents in the x_{2n} cycle structure factors is odd, namely 3). Furthermore, a single O_h–D_{6h}–O_h process changes an odd number (1 or 3) of vertices adjacent to a pivot vertex. Therefore a cube with the same adjacency relationships as the original cube can only be reached after an *even* number of O_h–D_{6h}–O_h processes. For this reason the topological representation of the O_h–D_{6h}–O_h process can only have cycles of even length and thus must be a bipartite graph [28]. Since a given cube has four *trans* complement pairs as possible pivots for the O_h–D_{6h}–O_h process, the connectivity (δ in Muetterties' notation [6]) of the cube in this process is 4. Since a given hexagonal bipyramid can go to two *hyperoctahedrally allowed* cubes by the O_h–D_{6h}–O_h process, the connectivity of the hexagonal bipyramid is 2. Since the products $J\delta$ for both the cube and the hexagonal bipyramid for this process are $(4)\,(8) = (2)\,(16) = 32$, this process is stereochemically closed [6].

B. Interconversion between the cube (O_h) and the square antiprism (D_{4d}) (the D_{4d}–O_h–D_{4d} process in Fig. 3b). This process involves a torsion around the four-fold axis of the square antiprism in the direction necessary to form the corresponding hyperoctahedrally restricted cube. Continuation of this torsion in the same direction gives the square antiprism with the four pairs of *trans* complements at the second antipodes (i.e. the *antipodally related* square antiprism). This process thus corresponds to the C_2 factor in the $P_4[P_2]\times C_2$

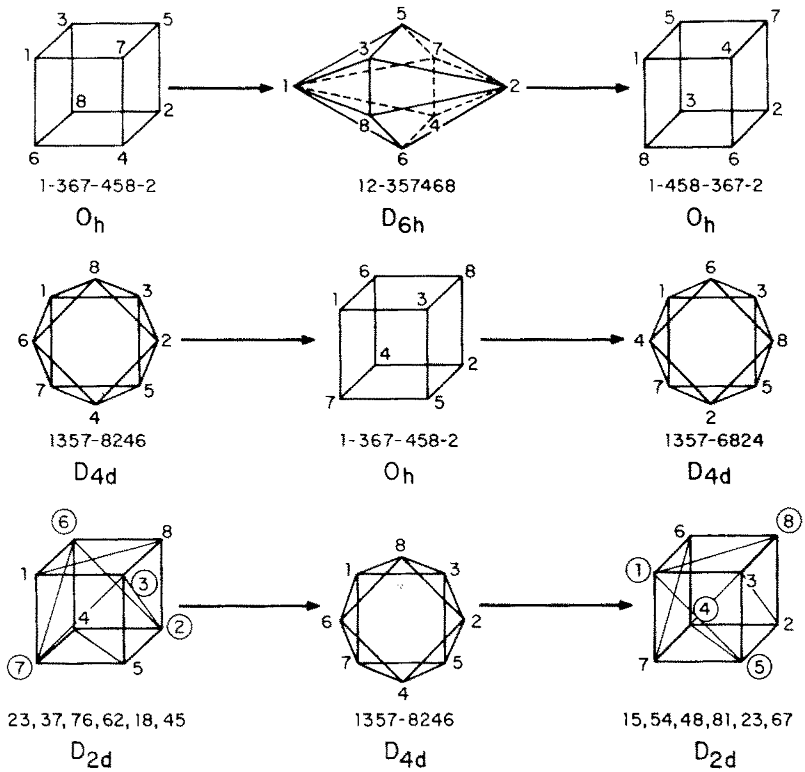

Fig. 3. The three processes for interconversions of eight-coordinate polyhedra discussed in this paper: (**a**) Top: O_h–D_{6h}–O_h process interconverting the cube and the hexagonal bipyramid; (**b**) Middle: The D_{4d}–O_h–D_{4d} process interconverting the square antiprism and the cube; (**c**) Bottom: The D_{4d}–D_{2d}–D_{4d} process interconverting the square antiprism and the D_{2d} dodecahedron. The labellings and symmetries of each polyhedron are indicated below the polyhedron

double group. Since for a given square antiprism, only one direction of twist satisfies the hyperoctahedral restriction, the connectivity of the square antiprism is 1. However, the intermediate cube has three different pairs of opposite faces. Each pair of opposite faces can be twisted either clockwise or counterclockwise to form pairs of antipodally related square antiprisms. Thus the connectivity of the cube in the D_{4d}–O_h–D_{4d} process is the product of 3 (the number of disjoint pairs of opposite faces in the cube) and 2 (corresponding to the two antipodally related square antiprisms) or 6. The products $J\delta$ are (8) (6) = 48 for the cube and (24) (1) = 24 for the square antiprism. However, the $J\delta$ product for the square antiprism must be doubled to 48 to allow for the two antipodally related square antiprisms. Therefore the D_{4d}–O_h–D_{4d} process is stereochemically closed. The cycle structure for the D_{4d}–O_h–D_{4d} process is $x_1^4x_2^2$ since the four vertices of one square face of the square antiprism are fixed (the x_1^4 factor) and the four vertices of the other square face oscillate past those of the stationary square face with a period of two in successive applications of the *hyperoctahedrally restricted* D_{4d}–O_h—D_{4d} process (the x_2^2 factor). This process is therefore an even permutation.

Since all improper symmetry operations of the square antiprism are odd permutations, the D_{4d}–O_h–D_{4d} process cannot interconvert enantiomeric square antiprisms.

C. Interconversion between the D_{2d} dodecahedron and the square antiprism (D_{4d}) (the D_{4d}–D_{2d}–D_{4d} process in Fig. 3c). This process is best viewed as a diamond-square-diamond motion [45] involving edges of the D_{2d} dodecahedron which arise from *primary* diagonals of opposite faces of the underlying cube. This process leads to the following results:
(1) The four vertices of degree 4 (1458 in Fig. 3c) and the four vertices of degree 5 (2367 in Fig. 3c) are interchanged in the D_{4d}–D_{2d}–D_{4d} process.
(2) Two primary diagonals become the two secondary diagonals and the two secondary diagonals become primary diagonals in the D_{4d}–D_{2d}–D_{4d} process.
(3) The belt of faces in the underlying cube containing the principal diagonal edges of the D_{2d} dodecahedron rotates 90° around the C_3 axis of the cube each time the D_{4d}–D_{2d}–D_{4d} process occurs. This period 3 belt rotation can, for example, be represented by the opposite faces bearing the *secondary* diagonals of the underlying cube *fixed in space* rotating in the following sequence: "back-front" to "left-right" to "top-bottom" and then back to "back-front".
(4) The permutation cycle structure of the D_{4d}–D_{2d}–D_{4d} process is x_2x_6 similar to an S_3 improper rotation [31] on a collection of eight points having appropriate symmetry.
(5) The D_{4d}–D_{2d}–D_{4d} process on a given D_{2d} dodecahedron must be applied *six* times before the original D_{2d} dodecahedron is reached again.
(6) The square faces of a given square antiprism can form two different D_{2d} dodecahedra depending upon which diagonals are added. The connectivity δ of the square antiprism for the D_{4d}–D_{2d}–D_{4d} process is therefore 2. Similarly, there are two possible pairs of primary diagonals of a given D_{2d} dodecahedron which can be removed to give two different square antiprisms. Thus the connectivity δ of the D_{2d} dodecahedron is also 2. The products $J\delta$ are therefore $(24)(2)=48$ for the square antiprism and $(48)(2)=96$ for the D_{2d} dodecahedron. However, as in the case of the D_{4d}–O_h–D_{4d} process, the $J\delta$ product for the square antiprism must be doubled to 96 to allow for the pairs of antipodally related hyperoctahedrally restricted square antiprisms. Thus the D_{4d}–D_{2d}–D_{4d} process is stereochemically closed.
(7) The x_2x_6 cycle structure of the D_{4d}–D_{2d}–D_{4d} process involves six transpositions [46], one for the x_2 factor and five for the x_6 factor. Furthermore, only an even number of successive D_{4d}–D_{2d}–D_{4d} processes can give a D_{2d} dodecahedron in which each vertex has the same adjacency relationships as the original dodecahedron (see item 1 above). Thus successive D_{4d}–D_{2d}–D_{4d} processes to give a D_{2d} dodecahedron with the same adjacency relationships as the original dodecahedron must necessarily involve an *even* number of *even* permutations, namely $4k$ (k is an integer) transpositions [46]. In the cycle index of the D_{2d} dodecahedron (Table 1) the terms containing $4k$ transpositions $(x_1^8+3x_2^4)$ correspond to the proper symmetry operations $E+C_2+2C_2'$ and the terms containing $4k+2$ transpositions $(2x_1^4x_2^2+2x_4^2)$ correspond to the improper symmetry operations

$2\sigma_d + 2S_4$. Since successive applications of the D_{4d}–D_{2d}–D_{4d} process can only effect permutations containing $4k$ transpositions on a *given* D_{2d} dodecahedron, the D_{4d}–D_{2d}–D_{4d} process cannot racemize such dodecahedra.

The three processes O_h–D_{6h}–O_h, D_{4d}–O_h–D_{4d}, and D_{4d}–D_{2d}–D_{4d} represent three of the six possible pairs of the four eight-coordinate polyhedra (cube, hexagonal bipyramid, square antiprism, and D_{2d} dodecahedron). The remaining three possible pairwise interconversions of eight coordinate polyhedra are forbidden at least under these hyperoctahedral restrictions for the following reasons:

(a′) Interconversion between the hexagonal bipyramid (18 edges) and the D_{2d} dodecahedron (18 edges) (a D_{6h}–D_{2d}–D_{6h} process) is forbidden because both polyhedra have the same number of edges. All of the allowed interconversions between eight vertex polyhedra (i.e. the O_h–D_{6h}–O_h, D_{4d}–O_h–D_{4d}, and D_{4d}–D_{2d}–D_{4d} processes outlined above) when applied repeatedly can be decomposed into processes involving alternating additions and subtractions of edges. The number of edges added or subtracted in each stage can be designated as Δe. Thus for the O_h–D_{6h}–O_h, D_{4d}–O_h–D_{4d}, and D_{4d}–D_{2d}–D_{4d} processes the Δe values are $18-12=6$, $16-12=4$, and $18-16=2$, respectively.

(b′) Interconversion between the hexagonal bipyramid (18 edges) and the square antiprism (16 edges) (a D_{6h}–D_{4d}–D_{6h} process) is forbidden since removal of even one of the necessary two edges from the hexagonal bipyramid to effect this process must give a vertex of degree 3. Therefore, the removal of edges from a hexagonal bipyramid cannot generate a square antiprism where all vertices have degree 4 even though a square antiprism has fewer edges than a hexagonal bipyramid.

(c′) Interconversion between the D_{2d} dodecahedron (18 edges) and the cube (12 edges) (an O_h–D_{2d}–O_h process) involves pairwise removal of six edges from the dodecahedron corresponding to the four primary and two secondary diagonals. For symmetry reasons, this pairwise removal of six edges should involve opposite faces of the cube. However, removal of the first pair of edges from the D_{2d}-dodecahedron towards forming a cube gives a square antiprism assuming that the more abundant primary diagonals connecting vertices of higher degree are removed in the first step. Therefore, the O_h–D_{2d}–O_h process can be decomposed into successive D_{4d}–O_h–D_{4d} and D_{4d}–D_{2d}–D_{4d} processes.

The relationship between the four eight coordinate polyhedra and the three allowed interconversion processes can be depicted by the following chain:

$$D_{6h} \underset{\Delta e=6}{\overset{\text{A}}{\rightleftarrows}} O_h \underset{\Delta e=4}{\overset{\text{B}}{\rightleftarrows}} D_{4d} \underset{\Delta e=2}{\overset{\text{C}}{\rightleftarrows}} D_{2d}.$$

For convenience, the letters above the arrows refer to the O_h–D_{6h}–O_h process (process A), the D_{4d}–O_h–D_{4d} process (process B), and the D_{4d}–D_{2d}–D_{4d} process (process C) as they are discussed above. The following observations can be made concerning this chain:

(1) The sequence of the polyhedra in this chain is *not* monotonic relative to their number of symmetry elements.

(2) The lowest energy process must be C, the D_{4d}–D_{2d}–D_{4d} process, since it is the only process in which both of the polyhedra involved can be formed only by s, p, and d orbitals of a central atom M in an ML_8 complex.

5. Topological Representations of Interconversions of Eight Vertex Polyhedra

A given hyperoctahedral graph H_4 leads to 120 enantiomeric pairs of the four eight vertex polyhedra considered in this paper. These include 8 pairs of cubes, 16 pairs of hexagonal bipyramids, 48 pairs of D_{2d} dodecahedra, and 48 pairs of square antiprisms (again doubling J in this case to allow for the two antipodally related square antiprisms). Polyhedra with connectivity two (e.g. the hexagonal bipyramid in the O_h–D_{6h}–O_h process and the D_{2d} dodecahedron in the D_{4d}–D_{2d}–D_{4d} process) which are also the end members of the interconversion chain given above can conveniently correspond to edges on the topological representations. (Strictly speaking, such connectivity two polyhedra correspond to the *midpoints* of such edges since in topological representations vertices (points) represent polyhedra and edges represent processes.)

These considerations lead to a topological representation of interconversions between hyperoctahedrally restricted eight vertex polyhedra enantiomeric pairs as a bipartite $K_{4,4}$ graph of hexagons as depicted in Fig. 4. The following features on this topological representation are of interest:
(1) The eight hexagons functioning as vertices in the $K_{4,4}$ graph correspond to the eight hyperoctahedrally restricted enantiomeric pairs of the cube.
(2) The 16 edges on the $K_{4,4}$ graph correspond to the eight hyperoctahedrally restricted enantiomeric pairs of the hexagonal bipyramid and thus represent O_h–D_{6h}–O_h processes (Process A).

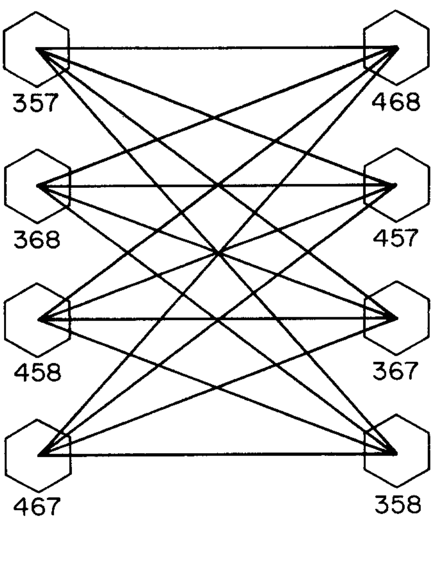

Fig. 4. The topological representation of the hyperoctahedrally restricted permutational isomerizations involving the eight-coordinate polyhedra discussed in this paper. The hexagons represent the eight cube hyperoctahedrally restricted enantiomeric pairs as indicated by the labels below each hexagon; the edges connecting the hexagons represent O_h–D_{6h}–O_h processes and the hexagonal bipyramidal intermediates; the vertices of the hexagons represent the square antiprisms; and the edges of the hexagons represent D_{4d}–D_{2d}–D_{4d} processes and the D_{2d} dodecahedra intermediates

(3) The $K_{4,4}$ graph is bipartite in accord with the fact the original cube can be reached only after an even number of O_h–D_{6h}–O_h processes.
(4) The six vertices on each of the eight hexagons correspond to the six square antiprism enantiomeric pairs that can be generated from a given hyperoctahedrally restricted enantiomeric pair of cubes through D_{4d}–O_h–D_{4d} processes. Antipodally related square antiprisms are located opposite each other in a given hexagon (i.e. three edges apart in "para" positions).

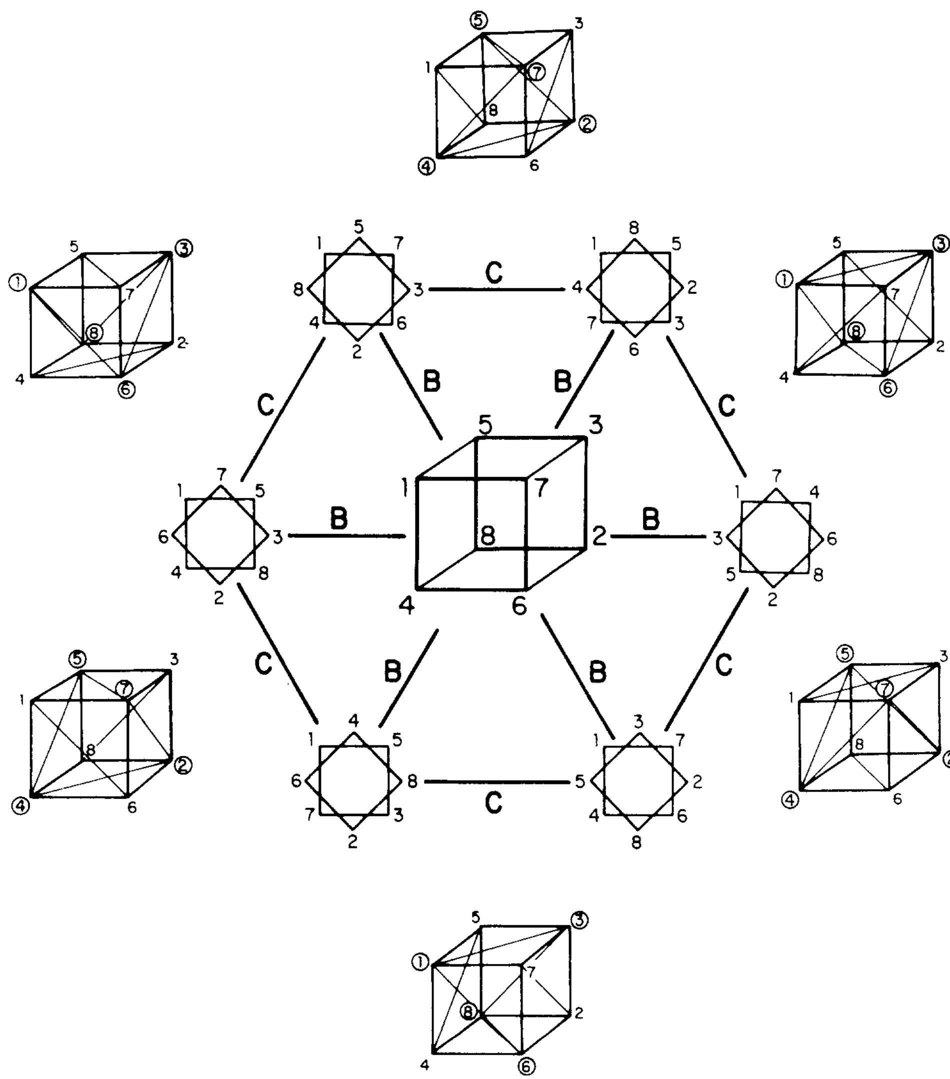

Fig. 5. Details of the hexagon in the topological representation corresponding to the 457 (1–457–368–2) cube. The spokes B represent D_{4d}–O_h–D_{4d} processes and the edges C represent D_{4d}–D_{2d}–D_{4d} processes as in Fig. 4. The D_{2d} dodecahedral intermediate involved in each of the six D_{4d}–D_{2d}–D_{4d} processes is depicted above the corresponding edge

(5) The six edges on each of the eight hexagons correspond to the six hyperoctahedrally restricted enantiomeric pairs of the D_{2d} dodecahedra that can be generated from the underlying cube corresponding to the hexagon in question.
(6) Details of the hexagon corresponding to the 457 cube are depicted in Fig. 5. If this hexagon is considered as a wheel, the spokes on the wheel correspond to D_{4d}–O_h–D_{4d} processes (Process B).
(7) Paths along the circumference of a given hexagon correspond to D_{4d}–D_{2d}–D_{4d} processes (Process C). This is the lowest energy eight-coordinate polyhedral interconversion. In terms of the topological representation depicted in Fig. 4 it is easiest to travel along the circumference of a given hexagon, much more difficult to jump to the center of the hexagon, and most difficult to travel along the edges of the $K_{4,4}$ bipartite graph to an adjacent hexagon.

6. The Group Structure of the Hyperoctahedrally Restricted Enantiomeric Pairs for the Various Eight Vertex Polyhedra

Klemperer [7] has discussed permutational isomers of polyhedra with n vertices in terms of their $n!/|R|$ right cosets where $|R|$ is the order of the proper rotational subgroup of the molecular point group and $n!$ corresponds to the order of the fully symmetric group P_n. Since $P_n = A_n \times C_2$ and A_n is a simple group [32] when $n \geqslant 5$, the symmetric group P_n cannot be factored into a direct product of the type $R \times S \times L$ or $G \times L$ where R is the pure rotation subgroup of the molecular point group, $S = C_1$ or C_2 depending upon whether the full molecular point group has an improper rotation axis (including a reflection plane $= S_1$), $G = R \times S$ is the full molecular point group, and L is a group containing $n!/|R|\,|S| = n!/|G| = |S|I$ elements corresponding to coset representatives [7] which are permutations giving another isomer where each different coset representative gives a different isomer. However, the $P_4[P_2]$ hyperoctahedral group, unlike the symmetric groups P_n ($n \geq 5$), is a soluble group [32] with 7 C_2 factor groups and one C_3 factor group $((2^7)(3) = 384)$. Furthermore, each of the eight-coordinate polyhedra considered in this paper have reflection planes and other symmetry operations involving improper rotation axes (S_n). Therefore for each of the eight-coordinate polyhedra, the spanning hyperoctahedral group $P_4[P_2]$ can be factored as follows:

$$P_4[P_2] = R \times C_2 \times L = G \times L. \tag{1}$$

The factor group L represents a group permuting the J hyperoctahedrally restricted enantiomeric pairs, which may also be regarded as coset representatives according to Klemperer [7]. Therefore $|L| = J = 384/|G|$.

We now examine the structure of the factor group L (Eq. 1) for the four eight-coordinate polyhedra of interest in terms of their generators as discussed in detail by Coxeter and Moser [47]. In considering the structure of the group L the distinction between direct and semidirect products [48] used by Woodman [49] is not made since the use of generators and relations makes the distinction unnecessary.

A. Cube. The group L is $C_2 \times C_2 \times C_2$ of order 8 with three generators a, b, and c of period 2 satisfying the following relationships:

$$a^2 = b^2 = c^2 = 1; \qquad ab = ba; \qquad ac = ca; \qquad bc = cb \tag{2}$$

If the cube 1–357–468–2 is taken as the reference cube, the generator a can represent the permutation (34), the generator b the permutation (56), and generator c the permutation (78). Each of these three generators represents a permutation of the type $x_1^6 x_2$ which is absent from the symmetry point group of the cube.

B. Hexagonal bipyramid. The group L is $C_2 \times D_4$ of order 16 with three generators a, b, and c of period 2 satisfying the following relationships:

$$a^2 = b^2 = c^2 = (ac)^2 = (ab)^2 = (bc)^4 = 1. \tag{3}$$

If the hexagonal bipyramid 12–345678 is taken as the reference hexagonal bipyramid, the generator a can represent the permutation (56), the generator b the permutation (13)(24), and the generator c the permutation (34)(56)(78). Then the products ab, ac, and bc become (13)(24)(56), (34)(78), and (1423)(56) of periods 2, 2 and 4, respectively.

C. D_{2d} dodecahedron. The group L is the product $(C_2 \times C_2 \times C_2) \times C_6$ of order 48. The $C_2 \times C_2 \times C_2$ factor is the same as the $C_2 \times C_2 \times C_2$ group of the underlying cube defined in Eq. 2. The generator of period 6 for the C_6 factor is the D_{4d}–D_{2d}–D_{4d} process.

D. Square antiprism. The group L is the product $(C_2 \times C_2 \times C_2) \times C_3$ of order 24. Again the $C_2 \times C_2 \times C_2$ factor is the same as the $C_2 \times C_2 \times C_2$ group of the underlying cube defined in Eq. 2. The additional C_3 factor arises from permutations of the three different pairs of opposite faces of the underlying cube that can be twisted to form different square antiprisms. If both antipodally related square antiprisms are considered then $L = (C_2 \times C_2 \times C_2) \times C_3 \times C_2$ and $|L| = 48$. The additional C_2 factor in this case arises from interchanges between clockwise and counterclockwise 45° twists of a given pair of opposite faces (the C_3 factor) of a given underlying cube (the $C_2 \times C_2 \times C_2$ factor).

A curious feature of this treatment is the involvement of the following three *non-isomorphic* groups of order 48:
(1) The product $(C_2 \times C_2 \times C_2) \times C_6$ which is the L group for the D_{2d} dodecahedron.
(2) The product $(C_2 \times C_2 \times C_2) \times C_3 \times C_2$ which is the L group for the square antiprism including the antipodally related pairs.
(3) The product $C_2 \times C_2 \times C_3 \times C_2 \times C_2 = O_h$ which is the point group of the cube.

7. Conclusion

The previous more general paper on the symmetries of coordination polyhedra [34] shows how the hyperoctahedral wreath product group $P_4[P_2]$ of order 384 spans as well as the fully symmetric group P_8 of order $8! = 40320$ all of the symmetries of all of the chemically important eight vertex polyhedra. This paper shows how the closely related doubled hyperoctahedral group $P_4[P_2] \times C_2$ of order 768 spans reasonable processes for the interconversions of the various eight-coordinate polyhedra as well as the permutational isomerizations of individual eight coordinate polyhedra. Restriction of isomerizations in eight-coordinate polyhedra to those involving permutations in $P_4[P_2] \times C_2$ allows construction of topological representations [6, 7] which are simple enough to be readily visualized. Thus a hexagon represents interconversions through square antiprismatic intermediates between D_{2d} dodecahedra derived from a given underlying cube. Furthermore, a $K_{4,4}$ bipartite graph with these hexagons as its vertices represents interconversions between such underlying cubes through hexagonal bipyramidal intermediates.

The hyperoctahedral wreath product group $P_4[P_2]$ differs from the fully symmetrical group P_8 by being soluble [32]. Therefore the group $P_4[P_2]$ can be represented as a product of cyclic factors. Thus hyperoctahedrally restricted permutation isomerizations have a group structure which is not generally found in unrestricted permutation isomerizations because $P_n = A_n \times C_2$ and A_n is simple [32] for $n \geq 5$.

The reduction of permutational symmetry from P_8 to $P_4[P_2]$ decreases the number of permutations by a factor of 105. A consequence of this reduction in symmetry is a loss of low energy pathways for the interconversion of enantiomeric eight-coordinate D_{2d} dodecahedra and square antiprisms. The existence of optically stable chiral but stereochemically non-rigid ML_8 complexes is therefore predicted. Thus a general conclusion from this work is that stereochemical non-rigidity need not imply optical lability.

References

1. For part IX of this series see reference 34
2. Longuet-Higgins, H. C.: Mol. Phys. **6**, 445 (1963)
3. Bauder, A., Meyer, R., Günthard, Hs. H.: Mol. Phys. **28**, 1305 (1974)
4. Gilles, J. M. F., Phillipot, J.: Intern. J. Quantum Chem. **14**, 299 (1978)
5. Cotton, F. A.: Acct. Chem. Res. **1**, 257 (1968)
6. Muetterties, E. L.: J. Am. Chem. Soc. **91**, 1636 (1969)
7. Klemperer, W. G.: J. Am. Chem. Soc. **94**, 6940 (1972)
8. Muetterties, E. L.: Inorg. Chem. **6**, 635 (1967)
9. Muetterties, E. L.: J. Am. Chem. Soc. **91**, 4115 (1969)
10. Brocas, J.: Top. Curr. Chem. **32**, 43 (1972)
11. Brocas, J.: Theoret. Chim. Acta. (Berlin) **21**, 79 (1971)
12. Brocas, J., Willem, R.: Bull. Soc. Chim. Belg. **82**, 469 (1973)
13. Brocas, J., Willem, R.: Bull. Soc. Chim. Belg. **82**, 479 (1973)
14. Gielen, M., Depasse-Delit, C., Nasielski, J.: Bull. Soc. Chim. Belg. **78**, 357 (1969)
15. Brocas, J., Gielen, M.: Bull. Soc. Chim. Belg. **80**, 207 (1971)
16. Gielen, M., Nasielski, J.: Bull. Soc. Chim. Belg. **78**, 339 (1969)
17. Gielen, M., de Clercq, M., Nasielski, J.: J. Organometal. Chem. **18**, 217 (1969)
18. Muetterties, E. L.: J. Am. Chem. Soc. **90**, 5097 (1968)
19. Gielen, M., Willem, R., Brocas, J.: Bull. Soc. Chim. Belg. **82**, 617 (1973)
20. Brocas, J., Fastenakel, D., Hicquebrand, J., Willem, R.: Bull. Soc. Chim. Belg. **82**, 629 (1973)

21. Gielen, M., Depasse-Delit, C.: Theoret. Chim. Acta (Berl.) **14**, 212 (1969)
22. Gielen, M.: Bull. Soc. Chim. Belg. **78**, 351 (1969)
23. Gielen, M., Mayence, G., Topart, J.: J. Organometal. Chem. **18**, 1 (1969)
24. Gielen, M.: Bull. Soc. Chim. Belg. **80**, 9 (1971)
25. Randić, M.: Croat. Chim. Acta **49**, 643 (1977)
26. Randić, M.: Intern. J. Quantum Chem. **15**, 663 (1979)
27. Trindle, C., Dutta, S. N., Bouman, T. D.: Intern. J. Quantum Chem. **11**, 627 (1977)
28. Behzad, M., Chartrand, G.: Introduction to the theory of graphs, Boston: Allyn and Bacon 1971
29. Grünbaum, B.: Convex polytopes. New York: Interscience Publishers 1967
30. Klemperer, W. G.: J. Chem. Phys. **56**, 5478 (1972)
31. Cotton, F. A.: Chemical applications of group theory. New York: Wiley-Interscience 1971
32. Budden, F. J.: The fascination of groups. London: Cambridge University Press 1972
33. Frucht, R.: Compositio Math. **6**, 239 (1938)
34. King, R. B.: Inorg. Chem., **20**, 363 (1981).
35. Biggs, N. L.: Algebraic graph theory. London: Cambridge University Press 1974
36. Pólya, G.: Acta Math. **68**, 145 (1937)
37. De Bruin, N. G.: Applied combinatorial mathematics, Chap. 5, E. F. Beckenback, Ed. New York: Wiley 1964
38. Harary, F., Palmer, E. M.: Graphical enumeration. New York: Academic Press 1973
39. Bechtell, H.: Theory of groups, Chap. 3. Reading, Massachusetts: Addison-Wesley 1971
40. Nourse, J. G., Mislow, K.: J. Am. Chem. Soc. **97**, 4571 (1975)
41. Kepert, D. L.: Prog. Inorg. Chem. **24**, 179 (1978)
42. King, R. B.: J. Am. Chem. Soc. **91**, 7211 (1969)
43. Shubnikov, A. V., Belov, N. V. and others,: Colored symmtry. New York: Macmillan 1964
44. Muetterties, E. L.: Inorg. Chem. **4**, 769 (1965)
45. Lipscomb, W. N.: Science **153**, 373 (1966)
46. Scott, R. F.: A treatise on the theory of determinants, p. 6. London: Cambridge University Press 1880
47. Coxeter, H. S. M., Moser, W. O. J.: Generators and relations for discrete groups. Berlin: Springer-Verlag 1972
48. Woodman, C. M.: Mol. Phys. **19**, 753 (1970)
49. Jansen, L., Boon, M.: Theory of finite groups. New York: Wiley 1967

Received August 4, 1980